

# Intumescent Flame-Retarded Building Parts Manufactured from Polyolefines as Well as from Composites of Polyolefines and Bismaleinimides

Heinrich Horacek

Free consultancy, A-4048 Puchenau, Am Wiesenrain 1

Received 24 June 2011; Revised 19 October 2011; accepted 27 November 2011

DOI 10.1002/app.36602

Published online in Wiley Online Library (wileyonlinelibrary.com).

**ABSTRACT:** Commercial intumescent flame retardants and intumescent compounds were tested as flame retardants for polypropylene. Their routes of decomposition were followed up by thermal gravimetric analysis, differential scanning calorimetry as well as thermal mechanic analysis and described by chemical formula, balances of weight, and heats of formation. These investigations showed that the combination of ammonium polyphosphate, polyols, and melamine exerted intumescence at 400°C and melamine was no blowing agent but reacted to melamine polyphosphate. Further they made clear that bisethylenediamine phosphate exerted intumescence at 350°C and degraded to piperazine phosphate. Intumescent flame-retarded building parts exemplified the advantage

of intumescent flame retardance by the time delay until they still fulfilled their function. F15 classification was achieved for thick walled intumescent polypropylene pipes and thin walled electrical boxes consisting of a flame-retarded glass reinforced bismaleinimide core and an intumescent polyolefine shell in furnace fire tests. The difference in temperatures inside and outside of the building parts was calculated and compared with measurements in fire tests. © 2012 Wiley Periodicals, Inc. *J Appl Polym Sci* 000: 000–000, 2012

**Key words:** differential scanning calorimetry (DSC); coextrusion; blowing agents; flame retardance; intumescence

## INTRODUCTION

Flame retardance will be guided by materials applied in the future and by new legislations. Legislation will push environmental friendly products, economy will favor low cost products which do not deteriorate the properties of the materials they are applied to.

Today 260 million tons of plastics are produced annually worldwide. The polyolefines have the highest share with 47% followed by polyvinylchloride with 12%. In the 60th polypropylene was a polymer without future. Today it is the worldwide most frequently applied plastic material with a market share of 18%.

Therefore, flame retardance of polyolefines and of polyolefine composites will be the challenge of the future. As there is no one flame-retardant FR for all plastics and as even for one plastic material different flame retardants are used for different applications the important task will be to find rules and measures for the development of the most appropriate flame retardants. The development of intumescent

flame retardants IFRs started with intumescent coatings. A decisive step was the incorporation of the IFRs in plastic materials in the 1950s.

Halogen-free intumescent flame retardance of polyolefines was already intensively investigated and described in the past.<sup>1–19</sup> In nearly all publications the intumescent flame-retarded polyolefines were classified according Ö-Norm 3800 or DIN 4102 as materials but not as building parts classified by time delay until their functions were still fulfilled.

1. The FRs tested comprised three groups: Inorganic compounds like ammonium polyphosphate APP and aluminum trihydrate ATH.
2. Mixtures of inorganic and organic compounds like APP with polyols, polyamines, and polyamides.
3. Reaction products of phosphoric acid with polyols, polyamines, and polyamides.

The FRs were investigated by thermal gravimetric analysis TGA, differential scanning calorimetry (DSC), and by thermal mechanic analysis (TMA).

A point in question was the role of melamine in intumescent mixtures: Does melamine really act as a blowing agent as claimed in recent literature?<sup>1</sup>

Correspondence to: H. Horacek.

TABLE I  
Applied Polymers

Product	Company	Type	Density g/cm <sup>3</sup>	Melt flow rate g/10 min	Vicat softening °C	
			ISO 1183	ISO 1133	ISO 306	
BE 50	Borealis	PP	0.905	3.0	160	B95
Daplen FM 533N	Borealis	PP	0.905	7.6	160	B92
Evatane 28-25	Arkema EVA	(28%Vac)	0.95	25	72	A40
Homide 250	HOS	BMI	0.5 (powder)		90	

The classification by time delay until the function was still fulfilled was common for building parts, for intumescent steel coatings, for fire doors, and for cable jacketing. As intumescence, the expansion under the influence of heat, is only possible when the glass or melt temperature of the polymer is surpassed the advantage of reduced heating rates due to better insulation can only be used in thick walled items with large gradients of temperature—temperature on the outer surface  $T_a$  much higher than the temperature on the inner surface  $T_b$ —or in composites with heat resistant polymers with high temperatures of decomposition  $T_{dec}$ . Therefore thick walled polypropylene pipes and thin walled composites made of a shell of intumescent polyolefines and a core of flame-retarded glass reinforced bismaleinimides were manufactured.

These samples were installed in a furnace heated according to the ISO curve and the time until they still fulfilled their function was determined in comparison with flame-retarded samples without intumescence. Because of foaming the parts were better insulated and the heating rates of the intumescent flame-retarded items were reduced. The samples ceased to fulfill their functions when the whole samples reached the temperature of fusion. In composites comprising intumescent polyolefines as shell and heat resistant polymers as core the time delay was defined by the temperature of the decomposing heat resistant flame-retarded polymer  $T_{dec}$  and the temperature of intumescence of the polyolefine  $T_i$  divided by the heating rate  $v$  of the sample:

$$t = (T_a - T_b)/v \dots \text{thick walled pipe} \quad (1a)$$

$$t = (T_{dec} - T_i)/v \dots \text{composite} \quad (1b)$$

When the outer temperature  $T_a$  of a thick walled pipe reached the temperature of fusion  $T_f$  followed by the temperature of intumescence  $T_i$ , then intumescence took place on the surface under foaming which reduced the heat conductivity, meanwhile the inner temperature  $T_b$  still remained below the heat distortion temperature. Due to better insulation the inner temperature raised at a reduced rate  $v$ . As soon as the inner temperature reached the temperature of fusion the sample collapsed. The time delay of collapse was estimated by eq. (1a).

In the case of a composite comprising an intumescent polyolefine as shell and a heat resistant polymer as core intumescence occurred at the temperature of intumescence  $T_i$ , the better insulation due to foaming reduced the rate of heating  $v$ . When the inner temperature of the composite reached the temperature of decomposition of the heat resistant polymer  $T_{dec}$ , then the composite was destroyed. The time lag was described by eq. (1b).

1. Therefore appropriate intumescent FRs should fulfill following requirements: Low temperature of intumescence  $T_i$  just above the melting temperature  $T_f$  of the polyolefines:  $T_i = T_f$
2. Stable and highly expanded char with good insulating properties and endotherm heat of decomposition as cooling as condition for a low heating rate  $v$ .

Commercial IFRs and chemicals were investigated by TGA, DSC, and TMA.

Complete balances of weights and heats of formation were set up and adjusted to the measurements in order to follow the steps of degradation and gases evolved.

Samples comprising polypropylene and FRs were manufactured by extrusion and injection molding and subdued Limiting Oxygen Index (LOI), Underwriters' Laboratories UL 94 and Cone Calorimeter tests.

## EXPERIMENTAL

### Materials

Polyolefines belong to the group of materials situated at the border line between mass and engineering plastics. For many applications a reduced combustibility is necessary. In Table I data of two species of polypropylene PP, of polyethylene vinylacetate EVA as well as those of bismaleinimide BMI were summarized. Bismaleinimides are thermosets and are 15 times more expensive than polyolefines therefore they occupy only niches.

As legislation will push environmental friendly FRs only halogen and heavy metal free FRs or chemicals were considered in Table II.

TABLE II  
Applied Flame Retardants

Product	Company	Chemical composition
Exolit 422	Clariant	Ammonium polyphosphate APP CAS 68333-79-9
Exolit IFR 23P	Clariant	APP + 30% Ammonium tartrate (%P=24 %N=13)
Hostaflam TP AP 745	Clariant	APP + Azodicarbonamide ?
Hostaflam TP AP 750	Clariant	"
Melapur P 46	Ciba	APP+ 20% PER, 30% melamine phosphate, 20% melamine cyanurate (%P = 16 %N = 26)
Spinflam MF 82 PP	Montefluos	APP+30% Triazinylpiperazine or EUF (ethylene urea formaldehyde (%P = 21 %N = 21)
Budit 3077	CW Budenheim	APP + 30% melamine formaldehyde (%P = 21,5 %N = 21,8)
Budit 3076	CW Budenheim	Budit 3077 + silicon oil (%P = 20,5 %N = 21)
Ethylenediamine diphosphate (EDADP) (%P = 24 %N = 11) $T_f = 175^\circ\text{C}$		
Ethylenediamine phosphate (EDAP) CAS 14852-17-6 (%P = 20 % N = 18) $T_{dec} = 240^\circ\text{C}$		
Amgard NK	Rhodia	(%P = 19.6 %N = 17.7)
Amgard EDAP	"	(%P = 19.6 %N = 17.7)
Amgard NP = Amgard NK + 2 nitrogen compounds N/P = 1,6		
Antiblaze NK	Albemarle	
Nord Min NK-27	Nordmann + Rassmann	
Degraded EDAP		
Piperazine diphosphate (PIDP) CAS 1951-97-9 (%N = 9,9, %P = 22,0) $T_f = 266^\circ\text{C}$		
Budit 3153 (CW Budenheim) Piperazine polyphosphate (%N = 11,4, %P = 25,2)		
Di(ethylenediamine) phosphate (DEDAP) CAS 7664-38-2 (%P = 16 %N = 27)		
Nord Min NP 28	Nordmann + Rassmann (%P = 15,5 %N = 27,5)	
Budit 3123	CW Budenheim	(%P = 16%N = 27)
Budit 3076 DC	"	(%P = 21%N = 20,5)
Reogard 1000	Great Lakes	(%P = 15.1%N = ?)
Antiblaze NP	Rhodia (Albright and Wilson)	(%P = 15.5%N = 27,5)
Degraded DEDAP		
Piperazine phosphate (PIP) CAS 1951-97-9 (%N = 15,2, %P = 16,8%) $T_f = 240^\circ\text{C}$		
Pori -risan 107	Nippon Chemical Ind. Corp	
Budit 3171	CW Budenheim (-N (CH <sub>2</sub> -CH <sub>2</sub> ) <sub>2</sub> N-PO <sub>1,5</sub> ) %N = 20, %P = 21,3	
Budit 3167 CW Budenheim (%P = 22 %N = 22) (60%DEDAP, 40%APP)		
Pentaerythritol phosphates		
NH 1197 Great Lakes Bicyclopentaerythritol phosphate BCPP CAS 5301-78-0, $T_f = 200^\circ\text{C}$		
Chargard 329	"	Dimelamine pentaerythritol phosphoric ester CAS 70776-17-9 (%P = 12,1 %N = 32,8)
Aluminum trihydrate Al(OH) <sub>3</sub> Apyral 60 (VAW aluminum AG) CAS 21645-51-2		
Melamine phosphate Fyrol MP (Akzo) CAS 20208-95-1		
Melamine cyanurate MC (Mitsubishi Petrochemical) CAS 37640-57-6		
Pentaerythritol (Perstorp) PER CAS 115-77-5 Dipentaerythritol DPER (Perstorp) CAS 126-58-9		

## EQUIPMENT

### Extrusion and injection molding

Samples for tests were manufactured in a twin screw extruder LSM 30/34 GL-9R from Leistritz Company and an injection molding machine ES 80 from Engel Company. During extrusion the output was 10 kg/h in all cases at a screw speed of 60–100 rpm. The tem-

peratures of extrusion were dependent on the polymer: 200–230°C for PP Daplen FM 533N (Borealis) and 140–180°C for EVA Evatane 28-25 (Arkema).

Pipes were manufactured on a pipe production line consisting of a ring nozzle with the diameters 285 and 249 mm, a calibration, a cooling device and equipment for transport. The pipes had an outer diameter of 29 cm and an inner diameter of 25 cm.

**TABLE III**  
Working Conditions

Injection pressure (bar)	Compression (bar)	Temp. of plastification (°C)	Temp. of mould (°C)
PP 400	1200	220	60
BMI 1000	700	210	200

Two single screw extruders Alpha 45 from Cincinnati were used for coextrusion. The coextruded IFR-EVA layer showed a thickness of 1.5 mm.

The polymeric materials EVA and PP were dried at 60 and 80°C for 2 h. The system was started with FR-PP BE 50 (Borealis) for the core. Once a consistent pipe was obtained the IFR-EVA material was fed to the extruder manufacturing the shell. The working temperature for the extruder providing the IFR-layer was about 195°C and was the same for both extruders.

Closed electrical boxes with the dimensions 100 × 100 × 55 mm<sup>3</sup> and a wall thickness of 3 mm were manufactured by injection moulding of FR-PP BE 50 and FR-BMI. Composites comprising a 1.5 mm core of FR-PP or FR-BMI and a 1.5 mm intumescent EVA shell were produced by two component injection molding under the conditions of Table III.

The FR-BMI formulation comprising 20% short glass fibers and 10% tribromomaleinimide was catalyzed by the addition of 1,5% 1,4 tert butylperoxypropyl benzene (Peroxid Chemie) and was post cured for 8 h at 200°C.

### Furnace

The fire tests were performed in a square shaped furnace with the dimensions of 1.5 m × 1.5 m × 0.5 m and a surface *F* of 7.5 m<sup>2</sup>, which was heated according to the ISO curve. The front side was protected either by a 15 mm silicate board Supalux V (Cape) or by a 5 mm steel panel which were insulated by 50 mm mineral wool RP XV (Rock wool). The heat flux *Q/F* was estimated by the mean consumption of 1 kg/h diesel oil with a heat of combustion of 42.000 kJ/kg and approximately amounted to 1.5 kW/m<sup>2</sup> according to eq. (2).

$$Q/F = 1 * 42.000 / (3600 * 7.5) = 1556 \text{ W/m}^2 \quad (2)$$

The heat flux per area *Q/F* was also calculated from the observed differences in temperatures between furnace and the front faces *dT* using eq. (3) for boards.<sup>20</sup>

$$Q/F = dT / (1/aw + d/lambda) \quad (3)$$

Iron Constantan thermocouples fixed on the surfaces of the silicate board and of the steel panel measured the temperatures. Then the differences *dT* between furnace and front side were determined. The *dT* values as well as the heat transfer number *aw* and the specific thermal conductivity *lambda* for silicate *a<sub>w</sub>* = 3 W/m<sup>2</sup> K, *lambda* = 0.13 W/m K and for steel *a<sub>w</sub>* = 25 W/m<sup>2</sup> K, *lambda* = 41 W/m K were introduced into eq. (3). To simplify matters no temperature dependences were taken into account. The calculated heat fluxes *Q/F* in Table IV were strongly time dependent for steel, a material with high heat conductivity, and changed from 500 to 6000 W/m<sup>2</sup>. For silicate, an insulating material, the calculated heat flux was more or less constant and showed a mean value of 1.2 kW/m<sup>2</sup>. For further calculations a mean heat flux *Q/F* = 1.5 kW/m<sup>2</sup> was used which was quite low in comparison with the heat flux of 50 kW/m<sup>2</sup> in the cone calorimeter.

Plastic pipes of the dimensions 29 cm outer diameter and 25 cm inner diameter were equipped with iron Constantan thermocouples in holes drilled in the inner wall fixed by water glass glue and glass fabric and placed in the furnace. In electrical boxes with the dimensions 10 × 10 × 5.5 cm<sup>3</sup> and a wall thickness of 3 mm thermocouples were glued on the inner wall of the boxes. The temperatures of the samples were observed in dependence of the temperature in the furnace.

The difference in temperature *dT* between outside and inside a pipe placed in a furnace with a heat flux of 1500 W/m<sup>2</sup> was calculated according to eq. (4).<sup>21</sup> The plastic pipe was characterized by a length *l* of 1 m, an inner radius *R<sub>i</sub>* of 12.5 cm, a thickness *d* of 2 cm, a heat conductivity *lambda* of 0.26 W/(m K), a surface *F*' = 2 × *P<sub>i</sub>* × *R<sub>a</sub>* × 1 = 0.91 m<sup>2</sup> and a horizontal perimeter to area factor *Hp/A* = 53 m<sup>-1</sup>.

**TABLE IV**  
Heat Flux *Q/F* of the Furnace for Insulated Front Faces of Silicate and Steel; Silicate: heat conductivity 0.13 W/(m.K); Steel: heat conductivity 41 W/(m.K)

Time (min)	T°C furnace	T°C 15 mm	dT°C	Q/F W/m <sup>2</sup>	T°C 5 mm	dT°C	Q/F W/m <sup>2</sup>
5	500	60	440	981	250	250	6250
10	660	105	555	1237	500	160	4000
15	700	150	550	1226	600	100	2500
30	800	270	530	1181	750	50	1250
45	870	330	540	1203	840	30	750
60	920	400	520	1159	900	20	500

$$dT = [(Q/F) * F'] * \ln(1 + d/R_i) / (\lambda * 2 * P_i * 1) \quad (4)$$

$$dT = [(1500 \times 0.91) \times \ln(1 + 2/12.5)] / (0.26 \times 2 \times 3.14 \times 1) = 124^\circ\text{C} \text{ PP-pipe without intumescence}$$

For the case of  $d/R_i < 1$  the expression  $\ln(1 + d/R_i)$  could be approximated by  $d/R_i$  so that eq. (4) degenerated to eq. (3) the equation for boards with  $R_a/R_i$  in addition under the condition of infinite  $a_w$  namely

$$dT = (Q/F) * F' / (2 * P_i * R_i * .1) * (d/\lambda) \\ = (Q/F) * R_a/R_i * (d/\lambda) \quad (3)$$

$$dT = 1500 \times 1.16 \times 0.02/0.26 = 134^\circ\text{C}$$

For an intumescent PP pipe a maximum expansion factor  $EF_{\max}$  of 10 was taken into consideration in eq. (5).<sup>22</sup>

$$dT = (Q/F) * F' * \ln[1 + (EF_{\max}/3) * d/R_i] / [( \lambda / EF_{\max} ) * 2 * P_i * 1] \quad (5)$$

$$dT = 1500 \times 0.91 \times \ln[1 + (10/3) \times 2/12.5] / [(0.26/10) \times 2 \times 3.14 \times 1] = 3567 \text{ intumescent PP-pipe}$$

The coextruded pipe comprised an intumescent shell of 1.5 mm thickness with a maximum of expansion  $EF_{\max} = 15$  and a nonintumescent core with a thickness of 18.5 mm. The contribution of the intumescent shell was calculated in 6a and that of the core in eq. (6b).

$$dT = 1365 * \ln[1 + 1.5 * 15 / (3 * 143.5)] / (2 * P_i * 0.26/15) \\ = 634^\circ\text{C} \text{ intumescent EVA-shell} \quad (6a)$$

$$dT = 1365 * \ln[1 + 18.5/125] / (2 * P_i * 0.26) \\ = 112^\circ\text{C} \text{ nonintumescent PP-core} \quad (6b)$$

Due to insulation the difference of temperature  $dT$  altogether amounted to  $746^\circ\text{C}$ .

The electrical boxes with  $Hp/A$  factor  $333 \text{ m}^{-1}$  and the dimensions  $10 \times 10 \times 5.5 \text{ cm}$  had a wall thickness  $d$  of 3 mm. Later they should be arranged on a gypsum board, therefore the relevant surface  $F'$  was that of the five-faced box  $F' = 0.1 \times 0.1 + 4 \times 0.1 \times 0.055 = 0.032 \text{ m}^2$ . To estimate the difference of temperature between the outer and the inner surface of the box eq. (3) was used under the assumption  $a_w$  infinite in eq. (3a) and (3b).

$$dT = 1500 * 0.032 * (0.003/0.26) \\ = 0.6^\circ\text{C} \text{ nonintumescent BMI core} \quad (3a)$$

The composite box comprised a 1.5 mm intumescent shell with  $EF_{\max} = 15$  which resulted in a  $dT =$

$21^\circ\text{C}$  and a 1.5 mm nonintumescent core with  $dT = 0.3^\circ\text{C}$  according to eq. (3a). Therefore the difference in temperature outside and inside was  $21.3^\circ\text{C}$ .

$$dT = 1500 * 0.032 * (0.0015 * 15) / (3 * 0.26/15) \\ = 21^\circ\text{C} \text{ intumescent EVA-shell} \quad (3b)$$

The calculations carried out demonstrated that a worth mentioning difference of inside and outside temperatures was only established in thick walled items.

In thin-walled parts a remarkable difference in temperature had to be accomplished by the construction of composites comprising a shell of low temperature of intumescence and a core of high temperature of decomposition.

The heats of combustion  $h_{\text{comb}}$  were investigated in a calorimeter according to DIN 51900 Teil 2 (1977) Heizwertbestimmung.

### DSC, TGA, and TMA apparatus

The ingredients were investigated by DSC, TMA, and TGA on a Mettler Toledo TMA/SDTA 840 with TGA/SDTA 851 Modul. In the case of TGA and DSC measurements the samples were placed in aluminum oxide crucibles of 900  $\mu\text{l}$  volume (ME 51119960) with 12 mm diameter covered by punctured lids. The TGA measurements took place under air with 50 ml/min rate and those of DSC under nitrogen with 80 ml/min at heating rates between 5 and 50 K/min. The TMA investigations were performed in aluminum oxide crucibles with 7 mm diameter and 4.6 mm height covered by 6 mm diameter lids in air at a heating rate of 50 K/min. TGA diagrams provided the residues  $R$  (%) dependent on temperature. By differentiation those temperatures  $T$  were obtained at which decomposition proceeded at highest speed.

When the samples were heated at different heating rates  $v$  (K/min) the energies of activation  $EA$  (kJ/g) could be calculated by following procedure: The inverse temperatures of maximum degradation  $1/T$  were plotted against the  $\lg v$  and the inclination  $dlgv/d(1/T)$  was determined.

By eq. (7) the energies of activation  $EA$  were calculated.

$$EA(\text{kJ/g}) = dlgv/d(1000/T) * [R/0.4343 * MW] \\ = dlgv/d(1000/T) * (19.15/MW) \quad (7)$$

$R$  = ideal gas constant (8315 J/mole) and  $MW$  = molecular weight (g/mole).

In case of fire the best possible result concerning the residue in air of a flame-retarded plastic material Rair(FR-plastic) was the added residues of the flame retardant in air Rair(FR) and that of the plastic under nitrogen  $RN_2(\text{plastic})$ .

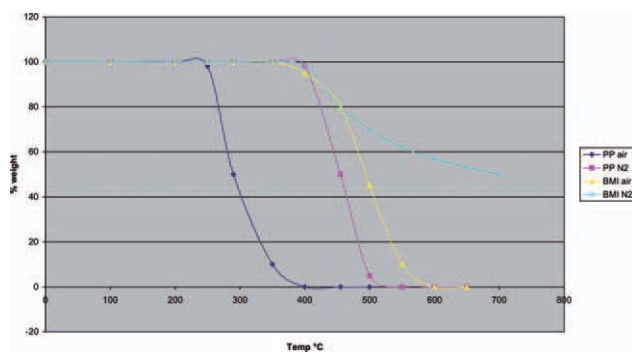


**Figure 1** TGA of PP and BMI in air and under nitrogen, 5 K/min. [Color figure can be viewed in the online issue, which is available at [wileyonlinelibrary.com](http://wileyonlinelibrary.com).]

$$R_{\text{air}}(\text{FRplastic}) = (100 - \% \text{FR}/100) \cdot R_{\text{N}_2}(\text{plastic}) + (\% \text{FR}/100) R_{\text{air}}(\text{FR}) \quad (8)$$

The worst result was the added residues of the flame retardant in air and that of the plastic in air.

The amount of FR demanded was always that amount of FR which guaranteed that the measured plastic residue was as high as that measured under nitrogen.  $R_{\text{air}}$  (plastic measured) =  $R_{\text{N}_2}$  (plastic). The higher the efficiency of the FR the lower the concentration needed to meet eq. (8).

From DSC data the heats of decomposition  $h_{\text{dec}}$  (kJ/g) and the temperatures of decomposition  $T_{\text{dec}}$  (°C) were obtained.

TMA measurements supplied the information on the expansion factor EF which was defined as the observed volume  $V$  divided by the volume of the untreated sample  $V_o$  minus 1:

$$EF = (V/V_o) - 1 \quad (9)$$

Further the onset temperatures of expansion, the temperatures of maximum expansion and the amounts of maximum expansion  $EF_{\text{max}}$  were determined.

The moles of gases  $n$  evolved from one mole of blowing agent was calculated with the aid of the ideal gas law when the maximum expansion  $EF_{\text{max}}$ , the specific volume  $V_o$  and the weight  $w$  of the investigated sample were known:

$$n = EF_{\text{max}} * V_o * w / 22,400 \quad (10)$$

High maximum expansion  $EF_{\text{max}}$  promised good insulating properties for IFRs.

### Limiting oxygen index

The LOI values were measured using a limiting oxygen index instrument on sheets of the dimension of  $100 \times 10 \times 4 \text{ mm}^3$  according ASTM D2863-77.

The test sample was mounted vertically with the ignition point at the upper end. First a concentration of  $\text{O}_2$  greater than that required to sustain burning was first determined. Then from that point the oxygen was lowered at a low rate until the flame was extinguished. Intumescent FRs evolved no or low burning gases as  $\text{H}_2\text{O}$ ,  $\text{NH}_3$ ,  $\text{CO}_2$ , and  $\text{N}_2$  therefore the oxygen concentration had to be increased to sustain burning. The efficiency was measured by the inclination of the LOI curve in dependence of concentration.

### Underwriter laboratories UL94

The UL-94 vertical test was carried out on samples with the dimensions of  $127 \times 12.7 \times 1.6 \text{ mm}^3$  according to ASTM D-635-77 and the three ratings V-2, V-1, and V-0 were established.

The best result was a V-0 classification at a low amount of IFR.

### Cone calorimeter

The samples, plates of 3 mm thickness, were tested in a FTT cone calorimeter according to ISO 5660-1 with a heat flux of  $50 \text{ kW/m}^2$ . The maximum heat release rate HRR max ( $\text{kW/m}^2$ ) and the time of maximum heat release  $t_{\text{max}}$  (s) were taken as a measure of efficiency.

## RESULTS

### TGA and DSC measurements

The polymers PP, EVA, and BMI as substrates for the flame retardants were characterized by TGA and DSC investigations. In Figure 1 the weight losses of PP and BMI were determined under nitrogen and air at a heating rate of 5 K/min. PP degraded without residue at  $280^\circ\text{C}$  in air and at  $445^\circ\text{C}$  under

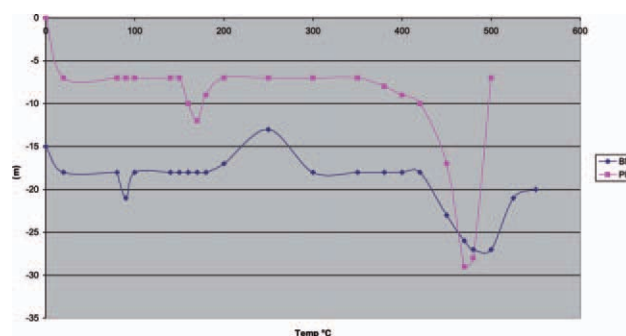


**Figure 2** DSC of PP and BMI in nitrogen, 20 K/min, PP:  $h_1 = 0,07 \text{ kJ/g}/T_m = 160^\circ\text{C}$ ,  $h_2 = 0.6 \text{ kJ/g}/T_{\text{dec}} = 470^\circ\text{C}$ , BMI:  $h_1 = 0,005 \text{ kJ/g}/T_f = 90^\circ\text{C}$ ,  $h_2 = -0.17 \text{ kJ/g}/T_{\text{cure}} = 250^\circ\text{C}$ ,  $h_3 = 0.25 \text{ kJ/g}/T_{\text{dec}} = 470^\circ\text{C}$ . [Color figure can be viewed in the online issue, which is available at [wileyonlinelibrary.com](http://wileyonlinelibrary.com).]

TABLE V  
DSC and TGA data of PP, EVA and BMI

Polymer	PP	EVA28%VA	BMI
MW	42	44	914
$T_f$ (°C)	160	72	91
$h_f$ (kJ/g)	0.07		0.005
$H_f$ (kJ/mole)	-76	179	-868.5
$h_{comb}$ (kJ/g)	-46.7	-33.5	-29.3
$v$ (K/min)	$T_{dec}$ (air/N <sub>2</sub> )	$T_{dec}$ (air/N <sub>2</sub> )	$T_c, T_{dec}$ (air/N <sub>2</sub> )
0	262/445		225, 495/460
5	287/456		232, 500/464
10	316/469		239, 505/468
20	341/483	275/325, 425/450	250, 515/470
40	360/510		260, 520/474
EA (kJ/g)	6	2.6	0.45/10
R (%)	0	80, 0	0/47
$h_{dec}$ (kJ/g)	0.6	0.78, 1.8	-0.17, 0.25
LOI	18	22	47

nitrogen. BMI resin decomposed in air at 500°C and in nitrogen at 465°C. Under air no residue was left but under nitrogen 45% of char sustained the heat.

In Figure 2 the heat changes were observed in dependence of temperature under nitrogen at 20 K/min heating rate for PP and BMI. PP melted at 160°C ( $h = 0.07$  kJ/g) and degraded at 450°C (0.6 kJ/g). BMI a thermoset melted at 90°C ( $h = 0.005$  kJ/g), cured at 250°C (-0.175 kJ/g) and partially degraded at 450°C (0.25 kJ/g). In Table V the data were collected for PP, BMI, and EVA. With these data in mind the route of combustion and decomposition could be set up in balances of weights MW (g/mole) and heats of formation H (kJ/mole). The quality of description was determined by the correspondence of experimental and calculated heats hex/cal (kJ/g) and experimental and calculated residues Rex/cal (%):

*Polyimide* = (2moles Diphenylmethanebismaleinimide + 1mole Methylenedianiline)

BMI = (2C<sub>21</sub>H<sub>14</sub>N<sub>2</sub>O<sub>4</sub> + 1C<sub>13</sub>H<sub>14</sub>N<sub>2</sub> = C<sub>55</sub>H<sub>42</sub>N<sub>6</sub>O<sub>8</sub>)

Combustion

$h_{comb} = -29.3$  kJ/g,  $T_{comb} = 500^\circ\text{C}$ ,  $R = 0\%$

F1: C<sub>55</sub>H<sub>42</sub>N<sub>6</sub>O<sub>8</sub> + 61,5O<sub>2</sub> = 55CO<sub>2</sub> + 21H<sub>2</sub>O + 3N<sub>2</sub>

MW (g/mole) 914 + 1968 = 2420 + 378 + 84

H (kJ/mole) -868,5 + -26.752,5 = -21.615 + -6.006

Decomposition

$h_{dec}$  ex/cal = 0,3/0,34 kJ/g,  $T_{dec} = 450^\circ\text{C}$ , Rex/cal = 47/46%

F2: C<sub>55</sub>H<sub>42</sub>N<sub>6</sub>O<sub>8</sub> = 8CO + 6NH<sub>3</sub> + 4CH<sub>4</sub> + 4C<sub>2</sub>H<sub>2</sub> + 35C

MW 914 = 224 + 102 + 64 + 104 + 420

H -868,5 + 312,5 = -888 + -276 -300 + 908

*Polypropylene*

Combustion

$h_{comb} = -46.7$  kJ/g,  $T_{comb} = 262^\circ\text{C}$ ,  $R = 0\%$

F3: C<sub>3</sub>H<sub>6</sub> + 4,5O<sub>2</sub> = 3CO<sub>2</sub> + 3H<sub>2</sub>O entfernen

MW 42 + 144 = 132 + 54

H -72 + -1965 = -1179 - 858

Degradation

$h_{dec}$  ex/cal = 0,6/0,55 kJ/g  $T_{dec} = 450^\circ\text{C}$ , EA = 250 kJ/mol, R = 0%

F4: (C<sub>3</sub>H<sub>6</sub>) = 0,5\*(0,6\*C<sub>5</sub>H<sub>10</sub>) + 0,5\*(0,5\*C<sub>6</sub>H<sub>12</sub>)

MW 42 = 0,5\*0,6\*70 + 0,5\*0,5\*84

H -76 + 22 = 0,3\*(-77,3) + 0,25\*(-123)

*Polyethylen vinylacetate*

EVA 0,28(C<sub>4</sub>H<sub>6</sub>O<sub>2</sub>)0,72(C<sub>2</sub>H<sub>4</sub>) = C<sub>2,56</sub>H<sub>4,56</sub>O<sub>0,56</sub>

Combustion

$h_{comb} = -33,5$  kJ/g,  $T_{comb} = 275^\circ\text{C}$ ,  $R = 0\%$

F5: C<sub>2,56</sub>H<sub>4,56</sub>O<sub>0,56</sub> + 3,42O<sub>2</sub> = 2,56CO<sub>2</sub> + 2,28 H<sub>2</sub>O

MW 44,2 + 109,4 = 112,6 + 41,0

H -179 -1479 = -1006 + - 652

Degradation

EVA  $h_{dec}$  ex/cal = 0,78/0,78 kJ/g,  $T_{dec} = 325^\circ\text{C}$ , EA = 115 kJ/mol, Rex/cal = 80/80%

F6: C<sub>2,56</sub>H<sub>4,56</sub>O<sub>0,56</sub> = 0,28 CH<sub>3</sub>COOH + C<sub>2</sub>H<sub>3,44</sub>

MW 44,2 = 16,8 + 27,4

H -179 + 34,5 = -123 + -21,5

EVA  $h_{dec}$  ex/cal = 1,8/1,8 kJ/g,  $T_{dec} = 450^\circ\text{C}$

Rex/cal = 0/0%

F7: C<sub>2</sub>H<sub>3,44</sub> = 0,28 C<sub>2</sub>H<sub>2</sub> gas + 0,72\*0,5C<sub>4</sub>H<sub>8</sub>

MW 27,4 = 7,28 + 20,16

H -21,5 + 78,5 = 0,28\*227 + 0,36\*-17

F8: EVA = 0,28(C<sub>2</sub>H<sub>2</sub> gas) + 0,28(CH<sub>3</sub>COOH) + 0,72\*0,5(C<sub>4</sub>H<sub>8</sub>)  $h_{dec}$  ex/cal = 2,58/2,57 kJ/g

MW (g/mol) 44,2 = 7,28 + 16,8 + 20,16

H (kJ/mol) -179 + 113,5 = 0,28(227) + 0,28(-439) + 0,72\*0,5(-17,5)

Flame retardants from Table II were investigated by DSC and TGA measurements and could be divided into following three groups:

1. Aluminum trihydrate ATH and ammonium polyphosphate APP were inorganic compounds without intumescence.

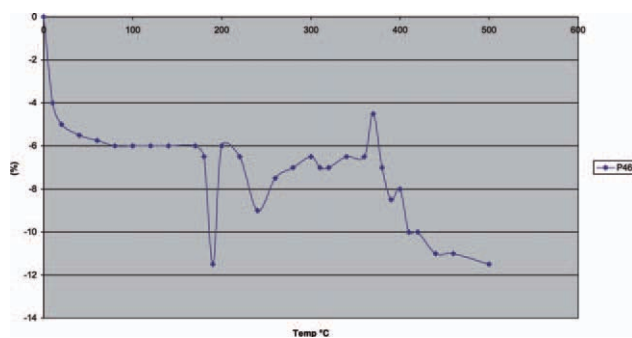


**Figure 3** DSC of Melapur P46 in  $N_2$ , 20K/min:  $h_1=0.05/190^\circ C$ ,  $h_2 = 0.14 \text{ kJ/g}/240^\circ C$ ,  $0.02 \text{ kJ/g}/290^\circ C$ ,  $h_3 = 0.04 \text{ kJ/g}/360^\circ C$ ,  $h_4 = 0.05 \text{ kJ/g}/400^\circ C$ . [Color figure can be viewed in the online issue, which is available at [wileyonlinelibrary.com](http://wileyonlinelibrary.com).]

- Intumescent commercial products comprised mixtures of APP with polyols as carbon sources like Exolit IFR, Melapur P46 and mixtures of APP, Pentaerythritol PER and Melamine M, well known as ingredients for intumescent paints. On their route of degradation APP and PER reacted to Bicyclopentaerythritol phosphate BCPP, which was also synthesized as a substance of reference by the reaction of phosphorus oxychloride and PER. Intumescent mixtures of APP with ethylene urea formaldehyde or polyamides were represented by Spinflam PP and Budit 3077.
- Reaction products of ethylene diamine and phosphoric acid. When ethylene diamine was titrated by phosphoric acid, the titration was stopped at definite pH values. After drying following salts were obtained:

pH	salt	
3	ethylenediamine diphosphate EDADP	$175^\circ T_f$
7	ethylenediamine phosphate EDAP	$240^\circ T_{dec}$
10	bisethylenediamine phosphate DEDAP	$200^\circ T_{dec}$

Under the influence of heat EDADP decomposed to APP, EDAP to piperazine diphosphate and DEDAP to piperazine phosphate.

In Figure 3 Melapur P 46 a mixture of 2 moles APP, 1mole PER, 1 moles MP and 0.5 mole MC was subjected to DSC analysis under nitrogen at a heating rate of 20 K/min. Intumescence at  $400^\circ C$  disturbed the DSC measurement on 100% powder P46 but less those on extruded samples with 25, 30, and 75% P46 in Table VI. Heat changes were observed:  $0.05 \text{ kJ/g}/190^\circ C$  recrystallization of PER,  $0.14 \text{ kJ/g}/240^\circ C$  fusion of PER and esterification with APP,  $0.02 \text{ kJ/g}/290^\circ C$  MP split off water,  $0.04/360^\circ C$  and  $0.05 \text{ kJ/g}/400^\circ C$ . Because of intumescence the zero line dropped down.

When a sample of PP comprising 25% P46 was investigated by DSC in Figure 4 the superposition of PP in Figure 2 and of Melapur P46 in Figure 3 was observed and following peaks were detected:  $0.045 \text{ kJ/g}/160^\circ C$  fusion of PP,  $0.015 \text{ kJ/g}/190^\circ C$  recrystallization of PER,  $0.035 \text{ kJ/g}/240^\circ C$  fusion and esterification of PER,  $0.005 \text{ kJ/g}/290^\circ C$  MP split off water,  $0.06 \text{ kJ/g}/360^\circ C$  decomposition of APP,MC, BCPP, and MPP (melamine pyrophosphate) as well as formation of melamine polyphosphate  $MHPO_3$ ,  $0.01 \text{ kJ/g}/400^\circ C$  intumescence and  $0.45 \text{ kJ/g}/450^\circ C$  decomposition of PP.

In Figure 5 the weight losses in dependence of temperature were investigated for samples with 100, 75, and 25% P46 in air at a heating rate of 20 K/min. The temperatures of maximum speeds of degradation were recognized at 240, 290, 360, 400, and  $450^\circ C$ .  $V$  the percentage of volatile compounds was equivalent to 100-R.

The weight and heat balance for P46, a mixture of 34% (1 m APP, 1 m PER), 33% (1 m MP), 19% (0.5 m MC), and 14% (1 mAPP), was set up using the heats of formation in Table VII. Few heats of formation  $H_f$  were available from the literature such as those for  $PER^{23}$  and  $ATH^{24}$  the others had to be calculated from the heats of combustion determined according to DIN 51900.

**TABLE VI**  
TGA in Air and DSC in Nitrogen of PP–P46 Extrudates, 20 K/min

	100%P46	75%P46	30%P46	25%P46	100%PP
T ( $^\circ C$ )	h (kJ/g)/R%	h (kJ/g)/R%	h (kJ/g)/R%	h (kJ/g)/R%	h (kJ/g)/R%
160	0/100	0/100	0.04/100	0.045/100	0.07/100
190	0.05/100	0.03/100	0.025/100	0.015/100	/100
240	0.14/95	0.1/95	0.04/96	0.035/97	/100
290	0.02/88	0.01/94	0.01/94	0.005/96	/50
360	0.04/75	0.1/82	0.04/88	0.06/95	/10
400	0.05/65	0.045/72	0.04/84	0.01/86	/0
450	55	0.15/59	0.48/52	0.45/55	/0
P46100% $h_{dec}$	0.3	$0.255/0.75 = 0.34$	$0.13/0.3 = 0.43$	$0.125/0.25 = 0.5$	/0



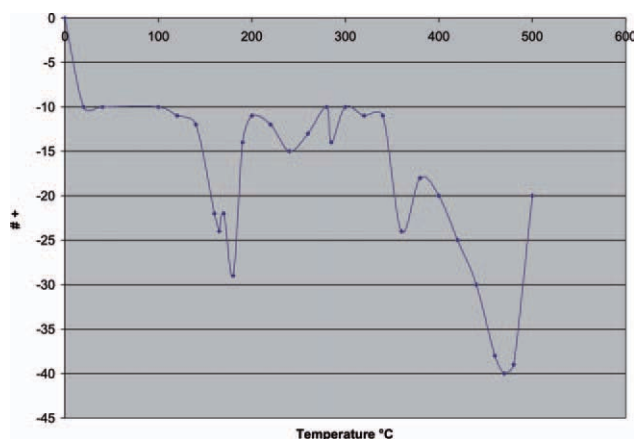


**Figure 4** DSC of PP with 25% Melapur P46 in  $N_2$ , 20 K/min:  $h_1 = 0.045$  kJ/g/160°C,  $h_2 = 0.015$  kJ/g/190°C,  $h_3 = 0.035$  kJ/g/240°C,  $h_4 = 0.005$  kJ/g/290°C,  $h_5 = 0.06$  kJ/g/360°C,  $h_6 = 0.45$  kJ/g/450°C. [Color figure can be viewed in the online issue, which is available at

#### Melapur P46

240°C,  $hex/cal = 0,14/(0,34*106/223)=0,16$  kJ/g,  $V = 0,34*23,8=8,1\%$ ,  $Rex/cal = 95/(100-V)=92\%$

F9: 34% (PER + APP =  $C_5H_9PO_5 + NH_3 + 2H_2O$ ) (Bicyclopentaerythritol phosphate)

MW 136 + 87 = 180 + 17 + 36

H -913 + -1085 + 106 = -1380 -46 - 484

290°C,  $hex/cal = 0,02/0,02$ ,  $V=0,33*4,0=1,3\%$ ,  $Rex/cal = 90/90,7\%$

F10: 33% (MP =  $M(H_4P_2O_7)_{0,5} + 0,5 H_2O$ )

MW 224 = 115 + 9

H -1312 + 16 = -1175 -121

360°C,  $hcal = 0,085$  kJ/g,  $V = 0,14*17,5=2,5\%$ ,  $Rex/cal = 75/88,2\%$

F11: 14% (APP =  $HPO_3 + NH_3$ )

MW 97 = 80 + 17

H -1085 + 58 = -981 - 46

360°C,  $hcal = -0,07$  kJ/g,  $V=0,34*16,1=5,5\%$ ,  $Rex/cal = 75/82,7\%$

F12: 26% ( $C_5H_9PO_5 = C_5H_5PO_3 + 2H_2O$ )

MW 180 = 144 + 36

H -1380 -47 = -943 - 2\*242

360°C  $hcal = 0,02$  kJ/g,  $V=0,33*4,0=1,3\%$ ,  $Rex/cal = 75/81,4\%$

F13: 31,5% ( $MH_2PO_{3,5} = MHPO_3 + 0,5H_2O$ ) (Melamine polyphosphate)

MW 215 = 206 + 9

H -1175 + 16 = -1038 -121

360°C,  $hcal = 0,19*692/255 = 0,52$  kJ/g,  $V = 0,19*50 = 9,5\%$ ,  $Rex/cal = 75/71,9\%$

F14: 19% [ $0,5(MC = Mgas + 3HOCN)$ ] (Cyanic acid)

MW 255 = 126 + 3\*43

H -993 + 692 = 50 - 3\*117

360°C,  $hcal = 0,15*-107/206 = -0,08$  kJ/g

F15: 15% [ $0,5(Mgas + HPO_3 = MHPO_3)$ ]

MW 126 + 80 = 206

H 50- 981- 107 = -1038

360°C over all  $hex/cal = 0,04/(0,08 -0,07+0,02 +0,52 -0,08) = 0,47$  kJ/g,  $Rex/cal = 75/71,9\%$

400°C Intumescence  $hex/cal = 0,05/-0,004$  kJ/g,  $Rex/cal = 65/68,1$

F16: 21% ( $C_5H_5PO_3 = C_4PO_{2,5} + 0,5H_2O + CH_4$ )

MW 144 = 119 + 9 + 16

H -943 + -3 = -750 -121- 75

$hcal = 0,64$  kJ/g

F17:

$2APP + PER + MP + 0,5MC = 5,5H_2O + 2NH_3 + 1,5HOCN + CH_4 + 1,5MHPO_3 + 0,5HPO_3$

+  $C_4,0,5P_2O_5$

MW  $2*97+136+224+127,5 = 99 + 34 + 64,5 + 16 + 309 + 40 + 119$

H  $2*-1085-931-1312-496,5+438,5 = 5,5*-242+2*-46+1,5*-117-75+1,5*-798+0,5*-981 + 0,5*-1500$

T (°C) 240 290 360 400

Sum of  $hex/cal = (0,14/0,16 + 0,02/0,02 + 0,04/0,47 + 0,05/-0,004) = 0,25/0,646$  kJ/g

$Rex/cal = 65/68,7\%$

At 400°C the char and comprised 65% experimental and 68,7% calculated residue consisting of  $MHPO_3$ ,  $HPO_3$ , and  $C_4,0,5P_2O_5$ .

Though the weight balance was in good agreement, the result of the heat balance, a small difference of two large figures, was in poor agreement.

The TGA and DSC data of the investigated FRs were listed in Table VII.

When the residues in air of pure FRs and of samples of good fire performance comprising PP and FRs were drawn in relation to the concentrations a straight lines as obtained in Figure 6 which followed eq. (8).

When the amounts of FRs were sufficient the residues of PP were the maximally possible, namely that under nitrogen.

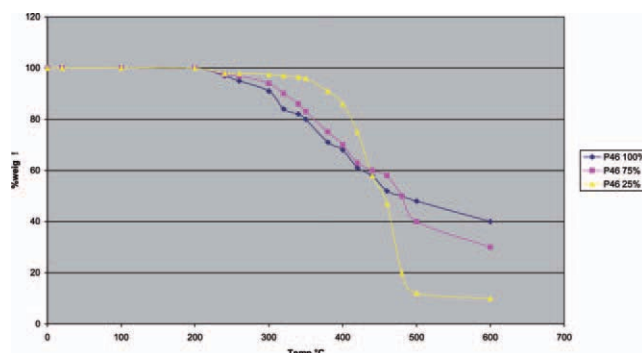


**Figure 5** TGA of Melapur P46 samples of PP comprising 100, 75, and 25% P46 under air, 20 K/min. [Color figure can be viewed in the online issue, which is available at

TABLE VII  
TGA and DSC Data of IFRs: Molecular Weight MW, Heat of Formation  $H_f$ , Heat of Combustion  $H_{comb}$ , Temperatures of Decomposition  $T_{dec}$  in Dependence of Heating Rate  $v$ , Energy of Activation EA, Residue R, and Heat of Decomposition  $h_{dec}$

FR	APP	ATH	PER	1mAPP/1mPER	4mAPP/1mPER	BCPP
MW (g/mole)	97	156	136	233	524	180
$H_f$ (kJ/mole)	-1085	-2570	-931	-2016	-5271	-1380
$H_{comb}$ (kJ/g)	-2,1	0	-20,3	-12,7	-6,8	-14,5
$v$ (K/min)	$T_{dec}$ °C	$T_{dec}$	$T_{dec}$	$T_{dec}$	$T_{dec}$	$T_f = 215$
0	325/620	300	300	240/340/400/600	235/260/350/500/540	$T_{dec}$
5	330/630	310	310	260/350/430/630	240/340/390/510//610	
10	340/650	330	330	280/360/440/660	250/350/417/530/675	
20	360/700	360	360	300/370/460/690	280/360/450/560/730	
40	370/770	380	380	320/390/465/750	300/390/480/580/760	310/340/360/500/600
EA(kJ/g)	1,5/1,1	0,6	0,6	0,45/0,57/0,54/0,54	0,2/0,4/0,2/0,1/0,2	
R (%)	85/20	1,1	0	73/60/55/10	88/76/71/60/15	90/80/75/65/50
$h_{dec}$ (kJ/g)	0,6/-	1,1	0,5	0,45/-0,2/-0,2/0,2	0,2/-0,1/-0,1/0,1/0,2	" -0,5/-0,5/0,15/0,2/0,3
MP	MC	EDAP	DEDAP	EDADP	PIP	PIPDP
MW(g/mole) 224	255	158	218	256	184	282
$H_f$ (kJ/g) - 1312	-993	-1370	-1559	-2628	-1354	-2533
$h_{comb}$ (kJ/g) -8,5	-11	-11	-17,2	-6,7	-15,4	-10
$T_{dec}$ $v = 20$ K/min	$T_{dec}$	$T_{dec}$	$T_{dec}$	$T_f = 175$	$T_f = 240$	$T_f = 266$
270/320/400/600/950	400	240/260/400/600	200/400/680	$T_{dec}$	$T_{dec}$	$T_{dec}$
R(%)96/91/61/27/0	0	76/65/55/10	95/68/23	175/200/325/400/680	250/330/400/540/600	266/330/400/540/600
$h_{dec}$ (kJ/g)	2,8	0,5/0,25/0,05/0,55	0,2/0,4/1,1	93/72/63/55/0	97/90/60/40/0	95/90/75/50/0
0,16/0,16/0,66/1,0/1,2				0,15/0,6/0,45/0,4/0,6	0,15/0,15/1,3/1,3/0,4	0,25/0,25/0,7/0,7/0,5

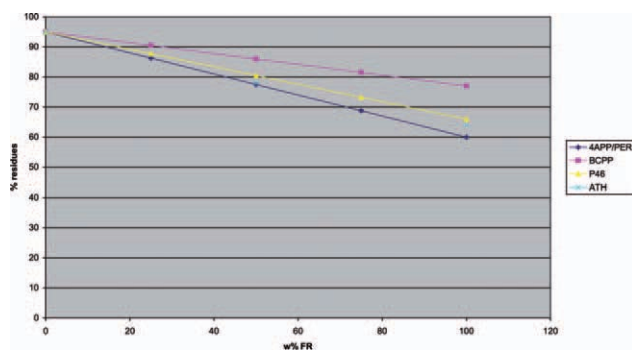


**Figure 6** Residues of samples comprising PP and sufficient amounts of FRs in air. [Color figure can be viewed in the online issue, which is available at

### TMA measurements

ATH evolved vapor at 300°C but no measurable expansion was observed. APP split off ammonia at 350°C and water at 400°C. The maximum expansion was 1,4 compared with 40 for a mixture of 4 moles APP, 1 mole PER, and 1 mole M in Figure 7. The  $EF_{max}$  for various molar combinations of nAPP, nPER, and nM as well as nAPP, nDPER, and nM were measured.<sup>25</sup> In Figures 8 and 9,  $EF_{max}$  showed a linear dependence on the molecular weight MW and followed the relations:

$$EF_{max} = 0,25 * [(nAPP - nM)/nPER] * MWAPP \quad (11)$$

$$EF_{max} = 0,20 * [(nAPP - nM)/nPER] * MWAPP \quad (12)$$

In defined limits the maximum expansion increased with the amount of ammonium polyphosphate APP and decreased with the amount of melamine M because M consumed APP reacting to melamine phosphate MP supporting the amount and stability of char.

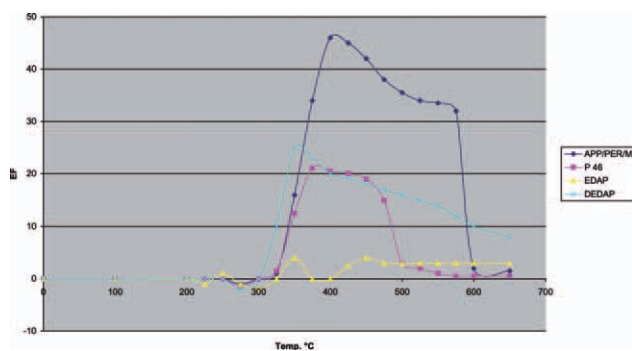


**Figure 7** TMA of Melapur P46, EDAP, DEDAP, and P46 a mixture of 3 m APP, 1 m PER, and 1 m M in air, 50 K/min, 0.02 N. [Color figure can be viewed in the online issue, which is available at wileyonlinelibrary.com.]

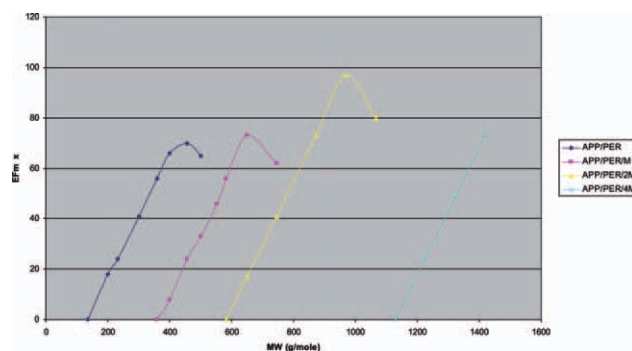


**Figure 8** Maximum Expansion  $EF_{max}$  as a function of MW molecular weights in molar mixtures of APP, PER, and M. [Color figure can be viewed in the online issue, which is available at wileyonlinelibrary.com.]

Using the ideal gas law the moles of gas evolved could be calculated. The powdery mixture of 1 mole APP (MW = 97) and 1 m PER (MW = 136 g/mol) had MW = 233g, a specific volume ( $V_o = 2.2 \text{ cm}^3/\text{g}$ ) and exerted a maximum expansion  $EF_{max} = 24$ . These figures inserted in eq. (10) lead to the result of 0.55 moles of gas.

$$n_{gas} = EF_{max} * V_o * w/22,400 = 0.55 \text{ mole} \quad (10)$$

At 400°C Melapur P46 comprising (2APP- 1M)/1PER=1 expanded by a maximum expansion factor 24 in experiment and 24,25 calculated in eq. (11). The char consisted of 1.5 M.HPO<sub>3</sub>, C<sub>4</sub>0,5P<sub>2</sub>O<sub>5</sub> and HPO<sub>3</sub>.

$$EF_{max} = 0,25 * 1 * 97 = 24,25 \quad (11)$$

EDAP built up an unstable foam exerting three peaks of expansion  $EF_{max} = 1$  at 250°C,  $EF_{max} = 4$  at 350°C, and  $EF_{max} = 3$  at 450°C.

At 350°C DEDAP foamed to an expanded char C<sub>3</sub>0,5P<sub>2</sub>O<sub>5</sub> at a maximum expansion of 21.

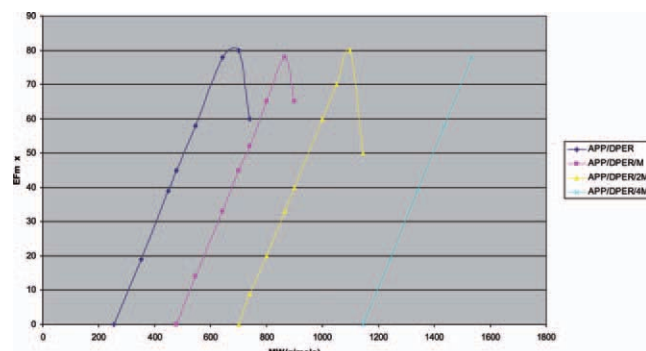


**Figure 9** Maximum expansion  $EF_{max}$  as a function of MW molecular weights in molar mixtures of APP, DPER, and M. [Color figure can be viewed in the online issue,

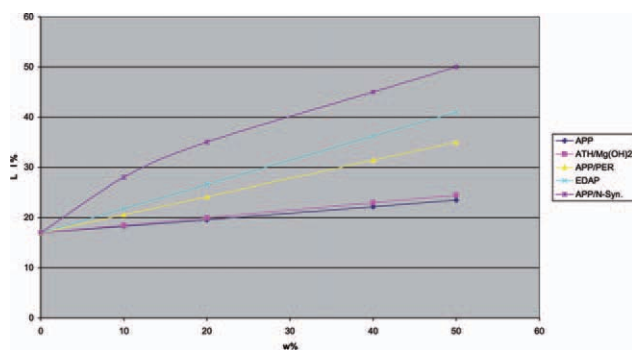


**Figure 10** LOI of PP-FRs samples. [Color figure can be viewed in the online issue, which is available at [wileyonlinelibrary.com](http://wileyonlinelibrary.com).]

TMA, DSC, and TGA investigations allowed formulations of the route of degradation for DEDAP and a mixture of PER and APP:

#### DEDAP

300°C; hex/cal=0,2/0,3 kJ/g; Rex/cal= 91/92%

F18:  $[\text{H}_2\text{N}(\text{CH}_2)_2\text{NH}_2]_2 \cdot \text{H}_3\text{PO}_4 = [\text{H}_2\text{N}(\text{CH}_2)_2\text{NH}_2]$

tiefgestellte 2.HPO<sub>3</sub> + H<sub>2</sub>O

MW 218 = 200 + 18

H -1559+65= -1252 + -242

320°C; hex/cal=0,23/0,23kJ/g; Rex/cal= 80/76% Piperazine polyphosphate

F19:  $[\text{H}_2\text{N}(\text{CH}_2)_2\text{NH}_2]_2 \cdot \text{HPO}_3 = \text{HN}-(\text{CH}_2)_4\text{-NH.HPO}_3 + 2\text{NH}_3$

MW 200= 166 +34

H-1252 +50 = -1110+ -92

330°C hex/cal= 0,2/0,2 kJ/g, Rex/cal=59/60%

F20:  $\text{HN}-(\text{CH}_2)_4\text{-NH.HPO}_3 = \text{C}_4\text{H}_4 \cdot \text{HPO}_3 + 2\text{NH}_3$

MW 166= 132 + 34

H -1110+50 = -968 + -92

350°C intumescence hex/cal= 0,1/0,1 kJ/g, Rex/cal= 39/49%

F21:  $\text{C}_4\text{H}_4 \cdot \text{HPO}_3 = \text{CH}_4 + 0,5\text{H}_2\text{O} + \text{C}_3\text{PO}_{2,5}$

MW 132= 16 + 9+ 107

H -968 +22 = -75 + -121+ -750

F22:  $[\text{H}_2\text{N}-(\text{CH}_2)_2\text{-NH}_2]_2 \cdot \text{H}_3\text{PO}_4 = 1,5\text{H}_2\text{O} + 4\text{NH}_3 + \text{CH}_4 + \text{C}_3 \cdot \text{PO}_{2,5}$  hex/cal = 0,8/0,86 kJ/g

MW 218 = 27 +68 +16 + 107

H -1559 +187 = -363- 184 -75 -750

1m PER and 1m APP

260°C; hex/cal=0,45/0,45 kJ/g; Rex/cal= 75/77%; EA= 0,45 kJ/g

F23:  $\text{APP} + \text{PER} = \text{C}_5\text{H}_9\text{PO}_5 + \text{NH}_3 + 2\text{H}_2\text{O}$  (BCPP)

MW 97 +136= 180 + 17 + 36

H -931+ -1085 +106 = -1380 + -46 + -484

350°C; hex/cal=-0,2/-0,2 kJ/g; Rex/cal= 60/60%; EA = 0.57 kJ/g

F24:  $\text{C}_5\text{H}_9\text{PO}_5 = \text{C}_5\text{H}_4 \cdot \text{HPO}_3 + 2\text{H}_2\text{O}$

MW 180 = 144 +36

H -1380 -47 = -943+ -484

Intumescence 430°C; hex/cal=-0,004/ -0,004 kJ/g, Rex/cal=55/51%, EA= 0,54kJ/g

F25:  $\text{C}_5\text{H}_4 \cdot \text{HPO}_3 = \text{C}_4 \cdot 0,5 \text{P}_2\text{O}_5 + 0,5\text{H}_2\text{O} + \text{CH}_4$

MW 144= 119 +9+ 16

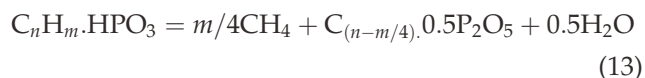
H -943 -3 = -750 + -121+ -75

F26:  $\text{PER} + \text{APP} = 4,5\text{H}_2\text{O} + \text{CH}_4 + \text{C}_4 \cdot 0,5\text{P}_2\text{O}_5$  hex/cal= 0.25/0.246 kJ/g

MW (g/mol) 136 +97 = 17 +81 +16+ 119

H (kJ/mol) -931 + -1085 +56 = -46 + -1089+ -75 + 750

These intumescent reactions indicate the common formula of intumescence, namely



#### Determination of LOI values

Samples were classified as self extinguishing when their LOI values were higher than 25.

Polypropylene without FR achieved a LOI value of 18 and bismaleinimide without glass and FR such one of 47. In Figure 10 flame-retarded PP samples without intumescence like those with ATH and APP occupied the lowest positions followed by APP/PER (4 m/1 m) and EDAP. On top were specimens comprising APP-Synergists like Melapur P46, Spinflam MF 80/PP, Exolit IFR 23, Hostaflam AP 745, Budit 3147 and a mixture of 40% APP and 60% DEDAP. See also Table VIII where the LOI values divided by concentration were tabulated. In principle the LOI measurements determined the amount of FR needed in order to achieve self-extinction.

#### Determination of V-0 rating according to UL 94 vertical test 1/16 inch

For V-0 rating commercial flame retardants were added to PP Daplen FM 553N in concentrations of 25–30%. See Table IX.

**TABLE VIII**  
LOI Values of FR-PP

LOI/%FR	FR
0,11	APP,ATH, MG(OH)2
0,22	Budit 3077 21,5%P, 21,8%N
0,25	1,5m MPP/ 1m DPER
0,29	Budit 3076DC 20,5%P, 21,0%N
0,29	7m APP, 1m DPER
0,24	4m APP, 1m PER
0,4	EDAP
0,41	DEDAP
0,46	Melapur P 46
0,6	Spinflam MF 82 66% APP, 34% EUF?
0,6	Hostaflam AP 750
0,7	Exolit IFR 66% APP, 34% Tartrat

**TABLE IX**  
**UL 94 Test of IFR**

FR	Company	Dosage %	UL 94	UL X-Y/Y <sup>a</sup>	Solubility g/l	Extraction% <sup>b</sup>
Melapur P46	CIBA	25	V-2	5-0/1	15	3,2
Exolit IFR 23	Clariant	25	V-2	05.01.2005	19	8,5
Spinflam MF 82/PP	Montefluos	25	V-2	05.01.2005	9	1,7
CP Flam	Vamp	25	N		28	
FR 910	Eurobrom	25	difficult	extrusion	44	
Charguard 329	Great Lakes	25	V-2	0-1/5	9	5,7
Amgard EDAP	Rhodia	25	N		52	6
Hostaflam AP 745	Clariant	25	V-2	5-0/3	22	8,3
Hostaflam TP AP 750	Clariant	25	V-2	04.01.2005	6	2,9
Budit 3077	C.W. Budenheim	25	V-2			
Daplen FM 553 PP-Homo	Borealis					

<sup>a</sup> X, number < 10 s; Y, number of dripping at 1/2 incineration.

<sup>b</sup> 24 h Soxhlet extraction by water.

The products based on ethylenediamine and phosphoric acid performed better because they had the advantage of lower temperatures of intumescence 350°C in comparison with products based on pentaerythritol and phosphoric acid with temperatures of intumescence at 400°C.

The mechanical properties of V-0 PP were summarized in Table X.

### Cone calorimeter tests

In Figure 11 the addition of IFRs to PP Daplen FM 533N and EVA Evatane 28-25 slowed down the rate of heat release RHH so that the maximum heat release was reduced and the time of maximum heat release was delayed. In Table XI the time delay of 3 mm thick plates amounted 3.3 min for IFR-PP and 2.5 min for IFR-EVA at a heat flux of 50 kW/m<sup>2</sup>

**TABLE X**  
**Mechanical Properties of V-0 Polypropylene**

Properties	Unit	Melapur P46		Spinflam MF 82/PP		Exolit IFR 23		Charguard 329		CP-Flam	
		Dosage pbw		0	25	0.	24	0	26	0	30
MFI (230/2,16)	g/10min	5	17	10	8	53	51	4,3	3,3	5	5,6
E-modulus	MPa	1600	2100	1700	2400			1640	3700	1000	1600
Flexural strength	MPa	47	57			56	51			23	12
Tensile strength	MPa			35	32			56,2	49,3		
Impact strength	kN/m2	20				32	16	22,5	4,5		40
Impact notched	kN/m2	4	-	2,5	1,8	4	4	0,9	0,9	9	4
LOI		18	32	17	37	18	38	18	34		
UL 94/1,6mm		V-0		V-0		V-0		V-0		V-0	
		Amgard EDAP		Hostaflam TP AP750		Budit 3077		Spinflam MF83		Hostaflam AP745	
Dosage		0	30	0	26	0	30	0	26	0	30
MFI (230/2,16)	g/10min	5	3	12	12			7	12	7	7
Tensile strength	kN/m2	20	18	30	27			25	37		24
Elongation	%			11	6						4
Charpy notched	kJ/m2			3,5	3,9						2
LOI		18	30	18	35	18	35	18	33	18	36
UL 94/1,6 mm		V-0		V-0		V-0		V-0		V-0	
Properties	Unit	BMI		BMI/10FR/20glass							
Dosage pbw											
MFI (230/2,16)	g/10min										
E-modulus	MPa	4.600	5.400								
Flexural strength	MPa	60	60								
Tensile strength	MPa	80	110								
Impact strength	kN/m2										
Impact notched	kN/m2										
LOI		47	45								
UL 94/16 mm		V-0	V-0								

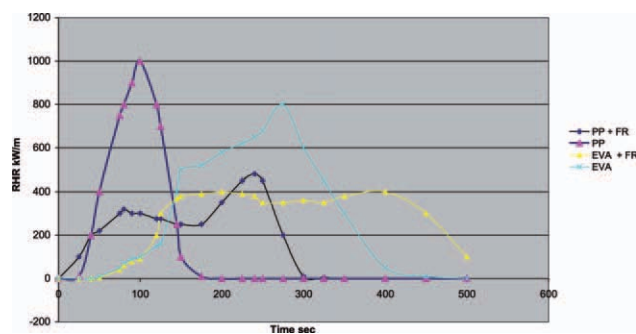


**Figure 11** Cone calorimeter tests of PP and EVA without and with 30% IFR (60% DEDAP and 40% APP). [Color figure can be viewed in the online issue, which is available at [wileyonlinelibrary.com](http://wileyonlinelibrary.com).]

which were comparable with 15 min obtained for the 20 mm thick IFR-PP pipe and 12 min for the coextruded IFR-EVA/PP pipe at a heat flux of 1.5 kW/m<sup>2</sup> in the furnace.

#### Determination of time delay until building parts still fulfilled their functions in a furnace

Polyolefine pipes with dimensions of an outer diameter of 29 cm and an inner diameter of 25 cm were extruded from PP BE 50 with 50% ATH and with 30% (60%DEDAP40%APP) with intumescence as well as coextruded with a PP core of a 18.5 mm thickness and a shell of 1.5 mm made of 60%EVA Evatane 25–28 and 40% (60%DEDAP 40%APP).

All three pipes were equipped with thermocouples fixed on the inner surface of the pipes and closed at both ends with mineral wool. They were placed in a 1125 m<sup>3</sup> furnace heated according the ISO-curve in such a way that one end crossed a 10 cm YTONG board.

In Figure 13 the temperatures were recorded as a function of time. The temperature of the furnace increased initially with a heating rate of 80 K/min. At 160°C PP changed from a solid to a melt.

At 450°C gasification started.

The samples comprising intumescent FRs changed their heating rate after the temperature of intumescence at 350°C was reached. Because of better insulation the heating rate was reduced from 45 K/min to 30 K/min. In Figure 13 the col-

**TABLE XI**  
Cone Calorimeter: Maximum Heat Release HRR Max and Time of HRR max

Sample	HRR max (kW/m <sup>2</sup> )	$t_{\max}$ (s)
PP	1000	100
PP 30%(60%DEDAP40%APP)	400	300
EVA	800	250
EVA 30%(60%DEDAP40%APP)	250	400

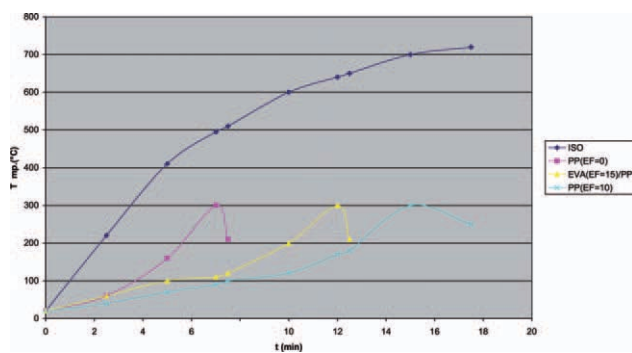


**Figure 12** Furnace test of PP pipes with a wall thickness of 20 mm according to the ISO curve. [Color figure can be viewed in the online issue, which is available at [wileyonlinelibrary.com](http://wileyonlinelibrary.com).]

lapse of the PP pipe flame retarded by the addition of 50%ATH (EF = 0) was observed after 6 min, the intumescent flame-retarded pipe sustained collapse until 15 min and the composite pipe of the same dimension with a 1.5 mm intumescent shell of highly concentrated IFR fulfilled its function until 12 min.

As the temperature on the surface of the pipes was unknown, only the difference of temperature in the furnace and inside the sample  $dT$  (furnace) could be observed:

FR-PP (without intumescence) 6 min,  $dT_{\text{cal}} = 124$  (eq. 4),  $dT$  (furnace) = 250°C,  $v = 250/6 = 41$  K/min

FR-PP (1.5 mm EVA EF = 15) 12 min,  $dT_{\text{cal}} = 746$  (eq. 6a, 6b),  $dT$  (furnace) = 400°C,  $v = 400/12 = 33$  K/min

IFR-PP (20 mm PP EF = 10) 15 min,  $dT_{\text{cal}} = 3.567$  (eq.5),  $dT$  (furnace) = 400°C,  $v = 400/15 = 27$  K/min

$$t = (T_a - T_b)/v = 400/27 = 15 \text{ min} \quad (1a)$$

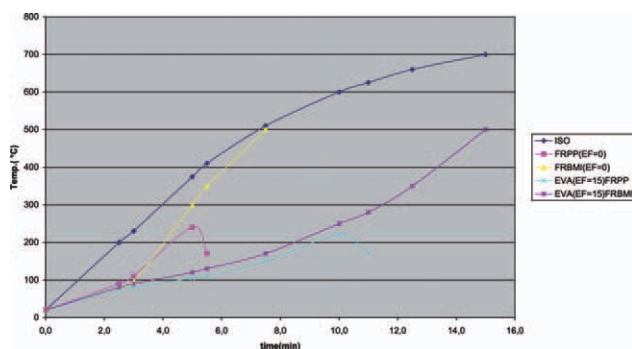


**Figure 13** Furnace test of electrical boxes with a wall thickness of 3 mm according to the ISO curve. [Color figure can be viewed in the online issue, which is available at [wileyonlinelibrary.com](http://wileyonlinelibrary.com).]

Four closed electrical boxes with the dimensions  $10 \times 10 \times 5.5 \text{ cm}^3$  and a wall thickness of 3 mm were manufactured by injection molding from flame-retarded FR-PP BE 50 with 50%ATH, from FR-Bismaleinimide resin (10% tribromomaleinimide, 20% short glass fiber). By two component injection molding composites comprising a 1.5 mm FR-PP as well as a 1.5 mm FR-BMI core and a 1.5 mm thick shell made of 60% EVA and 40% (60%DEDAP 40%APP).

The so manufactured boxes were arranged on a gypsum board on the front side of the furnace which was insulated by rock wool. The wires for the thermocouples were led through small holes in the board to the interior of the boxes. The boxes equipped with thermocouples were subduced a furnace test in Figure 14.

Four minutes were taken to reach the temperature of fusion at  $160^\circ\text{C}$  for the FR-PP box. The box made of FR-BMI reached in 6 min  $400^\circ\text{C}$  the temperature of decomposition.

The composite boxes achieved better results: IFR-EVA/FR-PP collapsed at  $160^\circ\text{C}$  after 9 min and the composite IFR-EVA/FR-BMI sustained destruction until 15 min.

FR-PP (without intumescence) 4 min,  $v = 160/4 = 40 \text{ K/min}$ ,  $dT_{\text{cal}} = 0.6^\circ\text{C}$  (eq. 3a),  $dT_{\text{(furnace)}} = 150^\circ\text{C}$

FR-BMI (without intumescence) 6 min,  $v = 250/6 = 42 \text{ K/min}$ ,  $dT_{\text{cal}} = 0.6^\circ\text{C}$  (eq. 3a),  $dT_{\text{(furnace)}} = 150^\circ\text{C}$

IFR-EVA/FR-PP (intumescent shell) 9 min,  $v = 300/9 = 33 \text{ K/min}$ ,  $dT_{\text{cal}} = 21.2^\circ\text{C}$  (eq. 3a, 3b),  $dT_{\text{(furnace)}} = 300^\circ\text{C}$

IFR-EVA/FR-BMI (intumescent shell) 15 min,  $v = 350/15 = 23 \text{ K/min}$ ,  $dT_{\text{cal}} = 21.3^\circ\text{C}$  (eq. 3a, 3b),  $dT_{\text{(furnace)}} = 300^\circ\text{C}$

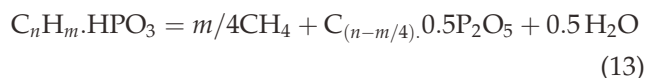
As the temperatures inside and outside the thin walled boxes were more or less the same, the time lag of the composites was determined by the difference of  $T_{\text{dec}} = 500^\circ\text{C}$  and  $T_i = 350^\circ\text{C}$  divided by the reduced heating rate of 10 K/min according to eq. (1b)

$$t = (T_{\text{dec}} - T_i)/v = 150/10 = 15 \text{ min} \quad (1b)$$

## SUMMARY

Intumescent flame-retarded polyolefines were investigated. The most common intumescent mixture comprising APP, PER, and M exerted intumescence at  $400^\circ\text{C}$  and astonished by the fact that M was not the blowing agent but consumed APP reacting to M polyphosphate and by this reduced intumescence

but increased and strengthened the char. For intumescence the common formula could be deduced from the investigated routes of degradation:



The reaction products of 2 moles ethylenediamine and 1 mole phosphoric acid degraded to piperazine polyphosphate and showed intumescence at  $350^\circ\text{C}$ . As a low temperature of intumescence was of advantage DEDAP flame-retarded samples achieved better results.

The experimental data obtained by TGA, DSC, and TMA allowed the description of routes of degradation by chemical equations, by balances of weights and by balances of heats of formation.

The advantage of intumescent flame retardance of building parts due to better insulation by foaming was demonstrated for the cases of thick-walled intumescent PP-pipes and thin walled electrical boxes composed of an intumescent polyolefin shell and a FR-bismaleinimide core.

In fire tests these samples reached a F15 classification. They sustained fire for 15 min. Simplified calculations of differences of temperatures on the surface and inside the samples were in accordance with measurements as far as available in principle.

The challenge of the future was seen in optimizing composites of heat resistant thermosets as core and highly insulating intumescent systems as shell for building parts with improved fire performance at reasonable costs.

Dedicated to my best friend the physicist Josef Lamprecht on the occasion of his 70th birthday.

## References

- Shun, Z.; Hongdian, L.; Lei, S.; Zhengzhou, W.; Yuan, H.; Jianxiang, N.; Weiyi, X. *J Macromol Sci Part A Pure Appl Chem* 2009, 46, 136.
- Lyons, J.W. *The Chemistry and Uses of Fire Retardants*; Wiley Interscience: New York, 1970; p 256.
- Ratz, R.; Sweeting, O. J. *J Org Chem* 1963, 1608.
- Vandersall, H. L. *J Fire Flammability* 1971, 2, 97.
- Brady, D. G.; Moberly, C. W.; Norell, J. R.; Walters, H. C. *J Fire Retardant Chem* 1977, 4, 150.
- Richly, J.; Matisowa-Rychla, L.; Vavrekova, M. *J Fire Retardant Chem* 1981, 8, 82.
- Ballistreri, A.; Montaudo, G.; Puglisi, C.; Scamporrino, E.; Vitalini, D. *J Appl Polym Sci* 1983, 28, 1743.
- Halpern, Y.; Mott, D. M.; Niswander, R. H. *Ind Eng Chem Prod Res Dev* 1984, 23, 233.
- Camino, G.; Costa, L. *Rev Inorgan Chem* 1986, 8, 1 and 2, 69.
- Montaudo, G.; Scamporrino, E.; Vitalini, D. *J Polym Sci Polym Chem Ed* 1993, 21, 3361.
- Morice, L.; Boubibot, S.; Leroy, J. M. *J Fire Sci* 1997, 15, 5, 358.
- Hilado, C. J. *Flammability Handbook for Plastics*, 5th ed.; Technomic Publ: Westport Conn., 1998; p 307.

13. Le Bras, M.; Camino, G.; Bourbigot, S.; Delobel, R. (Eds.) *Fire Retardancy of Polymers: The Use of Intumescence*; The Royal Society of Chem: Cambridge, 1998.
14. Shih-Hsuan, C.; Wun-Ku, W. *Polymer* 1998, 39, 10, 1951.
15. Gilbert, J. P.; Lopez Cuesta, J. M.; Bergeret, A.; Crespy, A. *Polym Degrad Stabil* 2000, 67, 437.
16. Lihua, W.; Jing, S. *J Macromol Sci Part B Phys* 2006, 45, 1.
17. Lomakin, S. M.; Dubnikova, I. L.; Zaikov, G. E.; Kozlowski, R.; Kim, G. M.; Michler, G. H. *GAK* 2007 Jg. 60 12 798.
18. Peng, H. Q.; Zhou, Q.; Wang, D. Y.; Ge, X. G.; Wang, Y. Z. *J Ind Eng Chem* 2008, 14, 589.
19. Vuillequez, A.; Lebrun, M.; Jou, R. M.; Youssef, B. *Macromol Symp* 2010, 290, 146.
20. Adolphi, G.; Adolphi, H. V. *Grundzüge der Verfahrenstechnik VEB Leipzig*, 1970, 115.
21. Ullmann 4.Aufl.Bd. 1 *Wärmeleitung und Wärmeübertragung* 120.
22. Horacek, H.; Pieh, S. *Polym Int* 2000, 49, 1106.
23. Kirk Othmer *Encyclopedia of Chemical Technology*, 3rd ed., Vol. 1; John Wiley and Sons: New York, 1978, p 778.
24. D'ans Lax, *Taschenbuch für Chemiker und Physiker* 1.Bd. 3. Aufl. Springer Verlag: Berlin, 1967; p 1.
25. Horacek, H. *J Appl Polym Sci* 2009, 113, 1745.